PAPER

A Linear Time Algorithm for Binary Fingerprint Image Denoising Using Distance Transform

Xuefeng LIANG[†], ***Nonmember and*** **Tetsuo ASANO**[†], ***Member***

SUMMARY Fingerprints are useful for biometric purposes because of their well known properties of distinctiveness and persistence over time. However, owing to skin conditions or incorrect finger pressure, original fingerprint images always contain noise. Especially, some of them contain useless components, which are often mistaken for the terminations that are an essential minutia of a fingerprint. Mathematical Morphology (MM) is a powerful tool in image processing. In this paper, we propose a linear time algorithm to eliminate impulsive noise and useless components, which employs generalized and ordinary morphological operators based on Euclidean distance transform. There are two contributions. The first is the simple and efficient MM method to eliminate impulsive noise, which can be restricted to a minimum number of pixels. We know the performance of MM is heavily dependent on structuring elements (SEs), but finding an optimal SE is a difficult and nontrivial task. So the second contribution is providing an automatic approach without any experiential parameter for choosing appropriate SEs to eliminate useless components. We have developed a novel algorithm for the binarization of fingerprint images [1]. The information of distance transform values can be obtained directly from the binarization phase. The results show that using this method on fingerprint images with impulsive noise and useless components is faster than existing denoising methods and achieves better quality than earlier methods.

key words: *impulsive noise, useless components, mathematical morphology (MM), Euclidean distance transform, integral image*

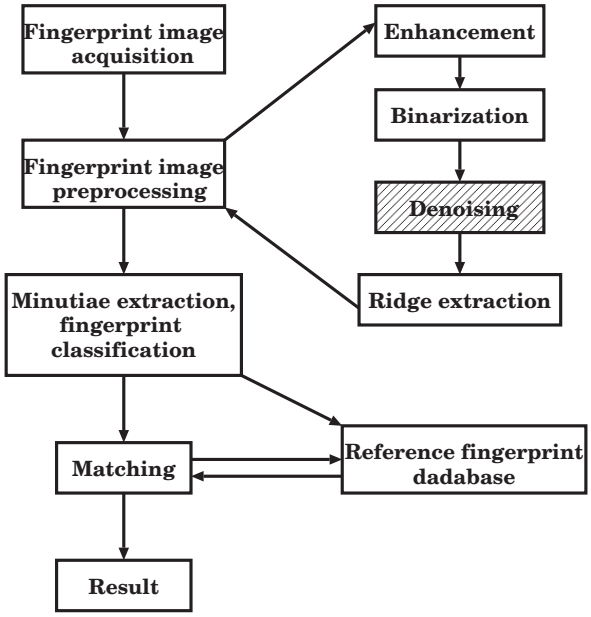

Fig. 1 A flowchart showing different phases of fingerprint analysis. The highlighted module shows the area of our work.

1. Introduction

Automatic fingerprint identification systems (AFISs) provide widely used biometric techniques for personal identification. Fingerprints have the properties of distinctiveness or individuality, and the fingerprints of a particular person remain almost the same (persistence) over time. These properties make fingerprints suitable for biometric uses. AFISs are usually based on minutiae (feature points) matching. Minutiae are local discontinuities of two types, terminations and bifurcations of the ridge flow patterns that constitute a fingerprint. These two types of minutiae are considered by the Federal Bureau of Investigation for identification purposes. A detailed discussion on all the aspects of personal identification using fingerprints can be found in Maltoni et al. [2]. AFIS based on minutiae matching involves different stages (see Figure 1 for an illustration):
1. fingerprint image acquisition;
2. preprocessing of the fingerprint image;
3. feature extraction (e.g. minutiae) from the image;
4. matching of fingerprint images for identification.

The performance of fingerprint recognition relies heavily on the quality of the input fingerprint image. However, in practice, due to skin conditions (e.g., wet or dry), sensor noise, incorrect finger pressure, and inherently low-quality fingerprints, a significant percentage of fingerprint images contain a lot of noise (see Figure 5(a)). Noises in fingerprint images fall into two categories: impulsive noise ("salt and pepper" noise) and useless components (see Definition 1). Note that useless components are often mistaken for the terminations that are an essential minutia of a fingerprint.

Several techniques have been developed for eliminating impulsive noise. Ratha, Chen, and Jain [3] implement a morphological opening in which the structuring element is a small box oriented according to the local ridge orientation. Wahab, Chin, and Tan [4] correct the binary image at locations where orientation estimates deviate from their neighboring estimates. This correction is performed by substituting the noisy pixels

Manuscript received March 09, 2005.
Manuscript revised August 22, 2005.

[†]The authors are with the School of Information Science, Japan Advanced Institute of Science and Technology, Nomishi, 923-1211 Japan.

according to certain oriented templates. Ikeda et al. [5] use morphological operators to enhance ridges and valleys in the fingerprint binary image. Since the first two methods consider the orientation, a fine selection of the directional filters is necessary. Although the third method employs an isotropic constructing element and as a result keeps the original shape of the fingerprint, the impulsive noise cannot be completely eliminated. However, the time complexity of these three is at least $O(N^2 \times d^2)$ for an image with $N \times N$ pixel entries and a filter whose radius is d. It is time consuming. In this paper, we first propose a simple and linear time complexity method, which employs generalized morphological operators (GMO) [16] based on distance transform and integral image [18], to eliminate the impulsive noise.

Up to now, there has been little in the literature with regard to eliminating the useless components. In order to do so, the structuring element chosen must have a good fit. There are three existing categories of methods for choosing the optimal or appropriate SEs. S. Fejes and F. Vajda's [6]–[8] algorithm employs the least mean square. It needs a reference image, which means this method will first do a training phase. But during fingerprint recognition process, it is unlikely that system could provide a reference image. Anelli, Loncaric and Dhawan's [9]–[11] algorithm uses a genetic algorithm (GA) to choose an optimal SE. Although GA really can find the optimal results with correct criteria , it is a time-consuming algorithm, and fingerprint recognition is a real time application. GA cannot satisfy this realistic restriction. Takuo Kikuchi and Shuta Murakami's [12] algorithm is based on the standard deviation of a linear SE with directionality. In their method, the length of the linear SE is determined by experience. In contrast, we define a condition for eliminating useless components based on the fact that the width of useless component must be less than the average width of finger ridges. We show how distance transform can be used as a measure for width and then design an algorithm to efficiently determine the size of the SE.

The rest of this paper is organized as follows. In Section 2, we briefly review a linear time Euclidean distance transform algorithm and the concept of generalized morphological operators. Section 3 describes a new way to represent structuring elements using Euclidean distance transform. Section 4 contains a discussion on a linear time generalized morphological operation on impulsive noise elimination. Section 5 discusses the algorithm for automatically eliminating useless components. Finally, we present our conclusions in Section 6.

2. Euclidean Distance Transform and Generalized Morphological Operators

2.1 A Linear-time Euclidean Distance Transform Algorithm

A two-dimensional binary image I of $N \times N$ pixels is a matrix of size $N \times N$ in which the entries are 0 or 1. The pixel in a row i and column j is associated with the Cartesian co-ordinate (i, j). For a given distance function, the *Euclidean distance transform* of a binary image I is defined in [13] as an assignment to each background pixel (i, j) a value equal to the Euclidean distance between (i, j) and the closest feature pixel, i.e., a pixel having a value 1. Breu et al. [13] proposed an optimal $O(N \times N)$ algorithm for computing the *Euclidean distance transform* as defined using Voronoi diagrams. Constructing and querying the Voronoi diagrams for each pixel (i, j) take time $\theta(N^2 \log N)$. But, the authors use the fact that both the sites and query points of the Voronoi diagrams are subsets of a two-dimensional pixel array to bring down the complexity to $\theta(N^2)$. In [14], Hirata and Katoh define *Euclidean distance transform* in an almost same way as the assignment to each 1 pixel a value equal to the Euclidean distance to the closest 0 pixel. The authors use a bi-directional scan along rows and columns of the matrix to find the closest 0. Then, they use an envelope of parabolas whose parameters are obtained from the values of the bi-directional scan. They use the fact that two such parabolas can intersect in at most one point to show that each parabola can occur in the lower envelope at most once to compute the *Euclidean distance transform* in optimal $\theta(N^2)$ time. In keeping with the above, we define two types of *Euclidean distance transform* values. The first one, $DT_{1,0}$, is the same as described above. The second one is $DT_{0,1}$, which is the value assigned to a 0 pixel equal to the Euclidean distance to the nearest 1 pixel. Using the results given in [14], we have the following fact:

Fact 1: Both $DT_{1,0}$ and $DT_{0,1}$ can be computed in optimal time $O(N^2)$ for an $N \times N$ binary image. Also, the values of both $DT_{1,0}$ and $DT_{0,1}$ are greater than or equal to 1.

2.2 Generalized Morphological Operators (GMO)

In mathematical morphology, signal transformations are called morphological filters, which are nonlinear operators that locally modify the geometrical features of signals. More details can be found in Serra and Soille [15].

Let $B \subset Z^2$ be a simple compact set of small size called structuring element. $\breve{B}$ is the reflection of B. F denotes a set of foreground pixels (black pixels) and

F^c denotes the background (white pixels). A morphological operation is a processing of the intersection of the SEs with F (or F^c). Therefore, when a large morphological kernel is used, the ordinary morphological operators have excessive operation (e.g., erosion, dilation).

For example, the morphological dilation of F by B can be generalized by combining the size of the intersection into the dilation process. In that sense, the dilation of F would be done if and only if the intersection between F and the shifted $\breve{B}$ is big enough. The obtained advantage of the generalized dilation is avoiding excessive dilation caused by small intersections. That is, the mass of an intersection should be big enough to cause a change.

The **generalized dilation** of F by B with strictness s is defined by:

$$F \overset{s}{\oplus} B = \{x : \#(F \bigcap \breve{B}) \geq s\}; s \in [1, min(\#F, \#B)]$$

where # denotes the cardinality of a set.

Ordinary dilation is obtained as a special case of generalized dilation when $s = 1$.

The **generalized erosion** of F by B with strictness s is defined by:

$$F \overset{s}{\ominus} B = \{x : \#(F^c \bigcap B) < s\}; s \in [1, \#B]$$

where it is assumed that $\#F < \infty$.

Similarly, the ordinary erosion is also obtained as a special case of generalized erosion when $s = 1$.

The properties of generalized morphological operators can be found in [16].

It is important to note that, using the generalized operators in existing algorithms with strictness greater than one may increase the resistivity of the algorithms to noise and small intrusions.

3. Description of Structuring Elements using Euclidean Distance Transform

Symmetrical and circular SEs play a fairly central role in mathematical morphology in the continuous plane, since they provide an isotropic treatment of the image. In the continuous domain, we use B_d to denote a circular SE whose radius is d, (see Figure 2). It is defined as:

$$B_d = \{b : d(b, 0) \leq d\} \tag{1}$$

Where $d(b, F)$ is the distance from SE center point $b(i, j)$ to the nearest pixel belonging to F. Then, erosion and dilation by B_d can also be expressed as the threshold of a distance value.

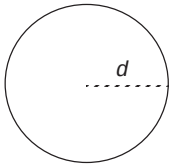

Fig. 2 Structuring element defined by distance value in continuous domain.

(a) 3×3 SE: $d = \sqrt{2}$ (b) Cross SE: $d = 1$

Fig. 3 Use of Euclidean distance value to describe "circular" SEs.

$$\begin{aligned} F \ominus B &= \bigcap \{F - b : d(b, F) \leq d\} \\ F \oplus B &= \bigcup \{F + b : d(b, F) \leq d\} \end{aligned} \tag{2}$$

The above equations show that morphological operators only deal with the pixels whose distance value is not greater than d.

However, for digital images, circular SE are rarely used because there is no "real" circular SE on a discrete lattice. The straightforward method to describe a SE is to pick up all pixels around the center point $b(i, j)$. However, this method has a drawback; whenever the center moves to the position $b(i', j')$, we have to update all other pixels in B. The process is naive and time consuming, and induce time complexity of the algorithm to $O(N^2 \times d^2)$ for an image of size $N \times N$ and a SE of radius d. Fortunately, we can employ Euclidean distance transform value to easily describe a "circular" SE in the discrete domain and further reduce time complexity of algorithm [17]. 3×3 SEs and cross SEs are much in use. In the following discussion, they will be used as examples to explain this principle, (see Figure 3).

In the discrete space, we assume each pixel is a unit square. For a 3×3 SE, the distance between a horizontal (or vertical) neighbor and the center is 1. Similarly, the diagonal neighbor is at distance $\sqrt{1^2 + 1^2} = \sqrt{2}$ from the center. This means every pixel whose distance from point $b(i, j)$ lies in $[1, \sqrt{2}]$ will be covered by a 3×3 SE centering on the point $b(i, j)$. Thus, we can easily denote 3×3 SE by $B_{d=\sqrt{2}}$ (Figure.3 (a)). In a corresponding way, since the cross SE only has horizontal and vertical neighbors, it can be denoted by $B_{d=1}$ (Figure.3 (b)). Next, the "circular" SEs denoted by Euclidean distance transform value are given.

$$\begin{cases} \text{SE with 5 pixels}, & B_{d=1}. \\ \text{SE with 9 pixels}, & B_{d=\sqrt{2}}. \\ \text{SE with 13 pixels}, & B_{d=2}. \\ \text{SE with 21 pixels}, & B_{d=\sqrt{5}}. \\ \text{SE with 25 pixels}, & B_{d=\sqrt{8}}. \\ \text{SE with 29 pixels}, & B_{d=3}. \\ \vdots & \vdots \end{cases} \tag{3}$$

4. Eliminating Impulsive Noise using Linear Time GMO

In practice, due to factors like skin conditions (e.g. wet or dry), sensor noise, or incorrect finger pressure, fingerprint images obtained from sensors often contain a lot of noise, which heavily affects the accuracy of further processing. The noises of fingerprint image have many shapes and directions. Thus, a fine selection of the directional ordinary morphological operators is required; a large morphological kernel may be also required. In such cases, the effects of denoising may damage the expected results due to extreme strictness of the ordinary morphological operators. So, we employ GMO in our system.

4.1 Advantages of GMO using Distance Transform

First, the GMOs have controllable strictness, and thus excessive erosion and dilation can be prevented. On the other hand, by controlling the strictness of a GMO, the GMO can adapt itself to the orientation and shape of fingerprint without adopting many directional operators.

Second, according to the properties of morphological operators, only the edge of a set F needs to be considered for computing these morphological operations. More accurately, equation 2 can be modified as follows,

$$\begin{aligned} F \ominus B &= F \bigcap (\partial(F) \ominus B) \\ F \oplus B &= F \bigcup (\partial(F) \oplus B) \end{aligned} \tag{4}$$

where $\partial(F)$ is the edge of F, that is the set of pixels of F with at least a direct neighbor not belonging to F and the distance transform value not greater than d. Assume l is the length of the contour of F (l is the cardinality of the set $\partial(F)$), then the computational complexity is reduced from $O(N^2 \times d^2)$ to $O(l \times d^2)$ for any SE of radius d. If the strictness of the GMOs is greater than 1, operators should count the number of intersected pixels between B and F^c (or $\breve{B}$ and F). Naive methods are dependent on the size of SEs. So, $O(l \times d^2) + N^2$ time is needed to check if the pixels belong to $\partial(F)$ by distance transform values.

Note that we usually use rectangular SE to do denoising (e.g. 3×3 SE, 2×3 SE, or 3×2 SE, etc.). Our method can further reduce $O(l \times d^2)$ to linear time by using integral image method.

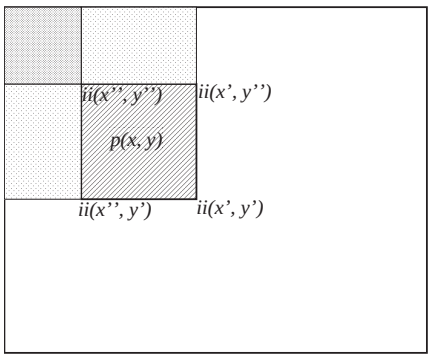

Fig. 4 Count inverse pixels of center using integral image.

4.2 Reducing Time Complexity by Integral Image

Integral Image was first used by Viola and Jones [18]. It is very similar to the summed area table used in computer graphics for text mapping [19]. The integral image can be computed from an image using a few operations per pixel. Once computed, any rectangular SEs can be computed at any scale or location in *constant* time.

The integral image at location (x, y) contains the sum of the pixels above and to the left of (x, y), inclusive:

$$ii(x, y) = \sum_{x' \le x, y' \le y} i(x', y'), \tag{5}$$

where $ii(x, y)$ is the integral image and $i(x, y)$ is the original image. Using the following pair of recurrences:

$$\begin{aligned} s(x, y) &= s(x, y-1) + i(x, y) \\ ii(x, y) &= ii(x-1, y) + s(x, y) \end{aligned}$$

where $s(x, y)$ is the cumulative row sum, the integral image can be computed in one pass over the original image. Then any rectangle sum can be computed in four array references.

Owing to GMO's strictness $s > 1$, during morphological operations, operators should know the number of intersected pixels between B and F^c (or $\breve{B}$ and F). Our strategy is to first represent the original binary image using an integral image (see Figure 4). When SE scans the point $p(x, y)$, we do the following operation.

$$n = ii(x', y') - ii(x'', y') - ii(x', y'') + ii(x'', y'')$$

where n is the number of background pixels in SE. For erosion, the state of the point $p(x, y)$ is converted if and only if $n \ge s$. It is similar to dilation.

From above, we get the following conclusion:

$$\begin{cases} O(N^2) & \textit{if rectangular SEs were used.} \\ O(N^2 \times d) & \textit{if isotropic SEs were used.} \end{cases}$$

In our method we employ rectangular SEs. So, the complexity of eliminating impulsive noise is **linear**.

4.3 Algorithm and Results

As the impulsive noise is fairly small and thin (specifically, one or two pixels wide in our case). And according to the property of GMO [16], strictness s must lie in interval $[2, \lfloor \#B/2 \rfloor]$. For a small SE, the integer midpoint $\lfloor \frac{2+\lfloor \#B/2 \rfloor}{2} \rfloor$ of the interval is reasonable strictness value. Therefore, a square SE of 3×3 pixels (corresponding to $d = \sqrt{2}$) with strictness of value 3 is used. The processing steps of this phase are as follows:

Input: A binary fingerprint image I of size $N \times N$ with impulsive noise.
Output: A binary image without impulsive noise.

1. Implement Euclidean distance transform for foreground pixels.
2. Represent binary image by integral image.
3. Pick up all pixels whose distance value are 1 or 1.414 and do generalized opening with strictness 3 using integral image on these pixels.

It is known computing times of both Euclidean distance transform and integral image are linear. In step 3, finding available pixels is exactly N^2. As analyzed in previous subsection, generalized opening using integral image can be done in $O(l)$ time. Therefore, the total time complexity is linear.

We tested 60 fingerprint images scanned from FUJITSU Fingerprint Sensor (model: FS-210u). These images are of size 300×300 and 500 dpi resolution. To make comparisons with our result easier, we list the average real computing times of these images in Table 1 and show result images in Figure 5, where OMO and GMO denote the methods based on ordinary and generalized morphological operators respectively. O. MO (Ratha) and O. MO (Wahab) are approaches proposed by Ratha et al [3] and Wahab et al [4] respectively. OMO results show broken ridges due to its excessive operation. For the Ratha, Chen, and Jain results [3], most impulsive noise has been removed, but computing time is longer than others, due to the need of finding the orientation of ridges. The Wahab, Chin, and Tan results [4] are fast but a little noise remains since only a few templates are employed. The approach of Ikeda et al. [5] needs special hardware, so we could not simulate it. Therefore, it is not shown in the Table 1 or Figure 5. From their paper, however, we learn that their approach does not remove the noise on the boundary of fingerprint ridges. In our results, the image is fairly clean and the fingerprint is less affected, because a GMO with strictness can adapt itself to the orientation and shape of fingerprint without adopting many directional operators. Moreover, another advantage of using GMO is that it needn't apply a closing to refill, as happens with the ordinary morphological operation. Thus, with GMO it is possible to carry out less operations. However, some useless components remain.

(a) Binary images with noise.

(b) Using OMOs.

(c) Using Ratha et al.'s approach.

(d) Using Wahab et al.'s approach.

(e) Using GMO by integral image.

Fig. 5 Results processed by various methods.

Table 1 The average real computing time among four methods to eliminate impulsive noise.

Method	Time (sec)
OMO	0.059
GMO	0.087
O. MO (Ratha)	0.323
O. MO (Wahab)	0.088

5. Automatically Choosing Appropriately-Sized Structuring Elements to Eliminate Useless Components

Owing to skin condition (e.g., wet) or incorrect finger pressure, some fingerprint images contain useless components, which are often mistaken for the terminations [17]; this makes it very difficult to correctly identify the minutiae relationships of a person's fingerprint image. Thus, AFISs recognize the fingerprint with useless components as a distinct print.

Definition 1: Useless Component is an object disjoint from other objects and whose largest width is less than the mean width of fingerprint ridges.

In order to eliminate useless components, a good SE is necessary. It is well known that the performance of mathematical morphology is heavily dependent on structuring elements (SEs). SEs have two aspects, size and shape. For denoising applications, the size of an SE is enlarged if membership values of the local area are uniform. If membership values of a local region are dispersed compared to other regions, minutiae may exist in that region. In this case, the SE must be small. For enhancement or feature extraction, in which expected objects either are distributed in the background with masses of other objects or are almost blended with background, the shape of the SE should approximate the target as closely as possible. So far, how to choose an optimal or adaptive SE is still a hot topic.

There are several methods to find the optimal or adaptive SEs, as described in the introduction. None of them, however, start with a definition of appropriate SEs. In contrast, we define a condition for eliminating useless components based on the width of the useless component, which must be less than the average width of finger ridges. We also employ distance transform and show how it can be used as a measure for width and then present our algorithm to efficiently determine the size of SEs.

5.1 Distance Transform and Ridge Width

Fingerprint images are characterized by almost equal width ridges (a small part of the image is shown in Figure 6). We will use this particular characteristic of fingerprint to estimate the size of SEs. Measuring the width for arbitrary shapes, however, is a difficult, nontrivial task. For easy understanding, we first model this problem in continuous domain to show how distance transform can be used to estimate the widths of ridges and useless components in fingerprint images and then, generalize it to the discrete domain.

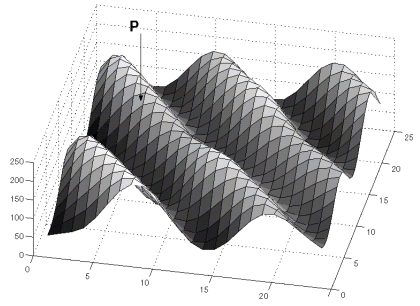

Fig. 6 Magnified view of a part of the gray scale topology of a fingerprint image.

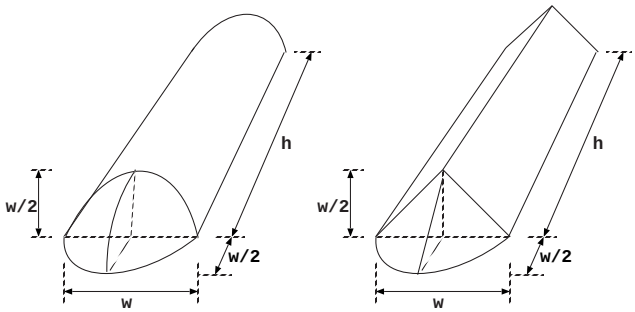

(a) 3D model of real ridge. (b) Distance transform 3D model.

Fig. 7 Diagrams of the 3D model.

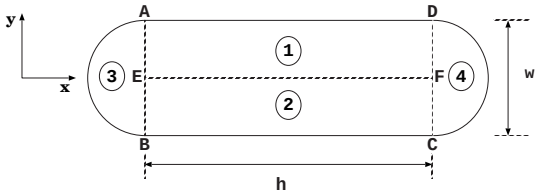

Fig. 8 Diagram for computing total distance value.

5.1.1 Model in the Continuous Domain

The fingerprint ridge can be modelled in 3D domain as shown in Figure 7(a). In the continuous domain, the image is a continuous function $f : (x, y) \rightarrow I\!R$. This function increases along a direction perpendicular to the ridge till it reaches the ridge top point, then decreases till it reaches the bottom. Since distance transform values are used to approximate to gray scale in our method, we obtain a distance transform 3D model as shown in Figure 7(b).

After projecting distance transform 3D model onto a plane, we get the planar diagram shown in Figure 8. We compute the total distance transform value of this shape. Consider this special geometric object of

width w and height h, with $h \gg w$. The medial axis of this object is given by the dot line segment $\overline{AB}$, $\overline{CD}$ and $\overline{EF}$. These dot line segments divide the geometric shape into four regions such that the nearest boundary line from any point in the region is determined. For instance, the region 1 has $\overline{AD}$ as its nearest boundary line and region 3 has $\widehat{AB}$ as its nearest boundary arc. The total distance transform value for region 1 is $\int_0^{\frac{w}{2}} \int_0^h (\frac{w}{2} - y)\ dxdy = \frac{1}{8}w^2h$. Similarly, the total distance transform value for region 3 is $\int_{\frac{\pi}{2}}^{\frac{3}{2}\pi} \int_0^{\frac{w}{2}} (\frac{w}{2} - r)r\ drd\theta = \frac{1}{48}\pi w^3$. So, the total distance transform value is:

$$\begin{aligned}\phi_{dt}(w) &= \frac{1}{8}w^2h \times 2 + \frac{1}{48}\pi w^3 \times 2 \\ &= \frac{1}{4}w^2h + \frac{1}{24}\pi w^3 \\ &= \frac{1}{4}w^2(h + \frac{1}{6}\pi w) \end{aligned} \quad (6)$$

From this result, we can find some relationship between the distance transform value and the width of the ridge. The length of the ridge, however, is fairly difficult to measure. Given this difficulty, it is reasonable to use the average distance transform value to measure ridge width. We first compute the area of the geometric object. The areas for region 1 and 3 are $\frac{1}{2}w \times h$, and $\pi(\frac{1}{2}w)^2 \times \frac{1}{2}$ respectively. So, the total area is:

$$\begin{aligned}\phi_S(w) &= \frac{1}{2}w \times h \times 2 + \pi(\frac{1}{2}w)^2 \times \frac{1}{2} \times 2 \\ &= wh + \frac{1}{4}\pi w^2 \\ &= w(h + \frac{1}{4}\pi w) \end{aligned} \quad (7)$$

The average distance transform value is equal to total distance transform value (equation 6) divided by area (equation 7). So,

$$\begin{aligned}E_{dt}(w) &= \frac{\frac{1}{4}w^2(h + \frac{1}{6}\pi w)}{w(h + \frac{1}{4}\pi w)} \\ &= \frac{1}{4}w\frac{h + \frac{1}{6}\pi w}{h + \frac{1}{4}\pi w} \\ &< \frac{1}{4}w \\ &\approx \frac{1}{4}w \qquad if \quad h \gg w \end{aligned} \quad (8)$$

In the definition of a fingerprint 3D model, the length is much greater than width. It implies that the average distance transform value can be approximated to one-fourth of the ridge width with a negligible error. So four times the average distance transform value is less than but almost equal to the average ridge width. Useless components are objects disjoint from other objects and their largest width is less than the mean width of the fingerprint ridges. This shows that the average distance transform value can be used as a good measure of estimating appropriate SEs. Our goal is to automatically determine appropriate "circular" SEs for eliminating useless components. The criteria is given by the definition of useless component (see Definition 1). So, more formally, we have the following lemma.

Lemma 1: When an isotropic SE satisfies the following condition:

$$max(w_{useless}) \leq 2d \leq mean(w_{ridge})$$

the useless components can be eliminated, but some eroded ridges of the fingerprint shall remain.

PROOF. According to the erosion of ordinary morphology, eroding an object can be found by intersecting all translates of the object by the reflection of the SE. As in our previous assumption, the diameter of isotropic SE is not less than the maximum width of the useless component. Then the object translated by the reflection of SE is too far to intersect any other translated object, i.e. $\bigcap\{F - b : b \exists B\} = \phi$. Thus, the useless components can be eliminated under such condition. The diameter $2d$, however, is not greater than the mean width of fingerprint. That means some wider portions, which are wider than SE, are not translated so far away that they can intersect each other. So, some of skeleton of the fingerprint remains.

5.1.2 Discrete Image and Distance Transform

In the discrete model, the co-ordinates are discrete given from the pixel locations. So, the observations from the previous subsection do not directly apply. But, the crucial observation from the previous subsection is that the average distance transform value approximates to one-fourth the width of the ridge. Then, an appropriate SE B can be obtained from the observation: Radius of the SE is less than but approximates to half the average width of the ridges. This observation still works in the discrete domain. However, the circular SE can move in an arbitrary direction in continuous domain. On the contrary, a "circular" SE only can move straight (in a horizontal or vertical direction) or diagonally with one step in the discrete domain. In this case, the SE radius must be remeasured by the same method as that used to measure ridge width instead of the simple radius d. We also need to consider the equal probability of moving straight or diagonally. Thus, the radius r of SE is the mean of radiuses in these two cases. Then, we have the following Definition:

Definition 2: An appropriate SE can be determined when half the average width of ridges is located in the corresponding interval.

$$\begin{cases} 2 \leq 2E_{dt}(w) < 2.828, & B_{d=1}. \\ 2.828 \leq 2E_{dt}(w) < 3, & B_{d=\sqrt{2}}. \\ 3 \leq 2E_{dt}(w) < 3.606, & B_{d=2}. \\ 3.606 \leq 2E_{dt}(w) < 4, & B_{d=\sqrt{5}}. \\ 4 \leq 2E_{dt}(w) < 4.243, & B_{d=\sqrt{8}}. \\ 4.243 \leq 2E_{dt}(w) < 4.472, & B_{d=3}. \\ \vdots & \vdots \end{cases} \quad (9)$$

where $E_{dt}(w)$ is the average distance transform value. B_d is a circular SE with radius d.

With this definition in place, we are in a position to design the algorithm in the next section.

5.2 Algorithm and Results

Our strategy is to take information from the original image I with useless components and the eroded image I_e by using the SE that satisfies Definition 2, in which useless components are eliminated completely but fingerprints cannot totally be deleted although they are affected to some degree. Then, we integrate fingerprint images I and I_e to restore the expected image I_r without useless components. More precisely, we establish a correspondence between the two images. The objects which do not correspond with any information in the eroded image I_e, are classified as useless components. We then eliminate them. The remaining objects, which have correspondences, are classified as fingerprint and remain in the final output image I_r.

To take care of non uniform ridge width across different image regions, we cut out sub-block of image region and pick up the minimal average distance transform value as criteria.

Input: A binary fingerprint image I of size $N \times N$ with useless components.
Output: A binary image without useless components.

1. Apply Euclidean distance transform on entire image;
2. **do for all** sub-block of the image I;
   Compute average distance transform value $E_{dt}(w_i)$;
3. Pick up $min(E_{dt}(w_i))$, then select appropriate SE B by definition 1;
4. Erode I by B;
5. Restore I_r by integrating I and I_e.

In this stage, we tested the same set of 27 images containing useless components as that used for the previous denoising stage (see Section 4.3). We also list the average real computing time in Table 2 and show the SEs chosen by different methods in Figure 9. The final results processed by other methods are almost the same, so Figure 10 only shows our result, where DT, LMS, GA and SD denote the methods based on distance transform, the least mean square, genetic algorithm and standard deviation, respectively. Time means the CPU time. Error means the number of useless components not eliminated.

Table 2 The average real computing time among four methods to eliminate useless components.

Method	Time (sec)	Error (num)
DT	0.063	0
LMS	0.34	1
GA	1.02	0
SD	0.374	0

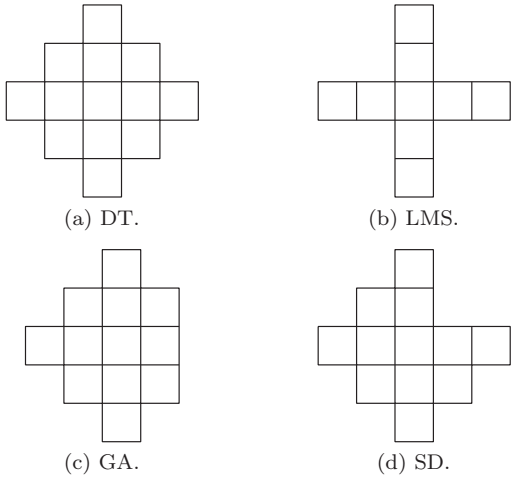

(a) DT. (b) LMS. (c) GA. (d) SD.

Fig. 9 SEs chosen by different methods.

The results show that our method (DT) is much faster than other three and works well. The least mean square method needs more time due to its training phase, and the chosen SE is not big enough, so that a few useless components remain. The genetic algorithm method takes the longest time, although it does find the optimal SE. But this computing time is unacceptable for a real time system. The standard deviation method can find an appropriate SE and run as fast as LMS. However, the length of the linear SE is determined manually, rather than automatically. Our method avoids these drawbacks. It runs fast and produces satisfactory results. Thus, it can be used with significant gains for fingerprint recognition in realtime applications.

6. Conclusion

We have developed a combinatorial linear time algorithm to eliminate impulsive noise and useless components from fingerprint images using Euclidean distance transform. There are two contributions. The first one represents binary fingerprint images and SEs by integral image and distance transform values, and reduce the time complexity of GMO from $O(N^2 \times d^2)$ to $O(N^2)$. The results are fairly clean and the fingerprint shapes are less affected. The second contribution is an algorithm for automatically determining an appropriate

(a) Images with useless components.

(b) Eroded images.

(c) Images without useless components.

Fig. 10 Results of eliminating useless components.

"circular" SE to eliminate useless components from fingerprint images exploiting the average fingerprint ridge width. We used Euclidean distance transform as a measure of width for determining the radius of SEs. One of the advantages of our method does not require parameters determined using experiences. Ordinary erosion with an appropriate SE only needs $O(l) + N^2$ time to eliminate useless components. So, the entire algorithm for fingerprint denoising is linear time. Note that, our denoising algorithm using distance transform has another distinct benefit. Please refer to Figure 1. The modules which precede and follow denoising are binarization and ridge extraction, respectively. We have developed a novel algorithm for binarization of fingerprint images [1], in which information about distance transform values can be obtained directly. And the ridge is the skeleton of the thick binary structures obtained from the binarization. Euclidean Distance Transform can be effectively used to find the skeleton [20]. Thus the same feature, distance transform, can be used for all binarization, denoising and ridge extraction operation which can save a lot of time in real applications.

7. Acknowledgment

Research for X.F. Liang was conducted as a program for the "Fostering Talent in Emergent Research Fields" in Special Coordination Funds for Promoting Science and Technology by Ministry of Education, Culture, Sports, Science and Technology. Research for T. Asano was partially supported by the same Ministry, Grant-in-Aid for Scientific Research (B) and Exploratory Research. The authors would like to deeply appreciate Arijit Bishnu and Kazunori Kotani for their helpful comments. FUJITSU LABORATORIES LTD. was extremely helpful in providing devices for our research.

References

[1] X.F.Liang, A. Bishnu, T.Asano, "A near-linear time algorithm for binarization of fingerprint images using distance transforms". Proc. The 10th IWCIA, pp. 197-208, 2004.
[2] D. Maltoni, D. Maio, A.K. Jain and S. Prabhakar, Handbook of Fingerprint Recognition, Springer-Verlag, New York, 2003.
[3] N.K. Ratha, S.Y. Chen and A.K. Jain, "Adaptive Flow Orientation-Based Feature Extraction in Fingerprint Images", Pattern Recognition, Vol. 28, no. 11, pp. 1657-1672, 1995.
[4] A. Wahab, S.H. Chin and E.C. Tan, "Novel Approach to Automated Fingerprint Recognition", IEEE Transactions on Pattern Analysis and Machine Intelligence, Vol. 145, no. 3, pp. 160-166, 1998.
[5] N. Ikeda et al., "Fingerprint Image Enhancement by Pixel-Parallel Processing", Proc. Int. Conf. on pattern recognition (16th), Vol. 3, pp. 752-755, 2002.
[6] S.Fejes, F.Vajda, "Simplified Adaptive Approach to Efficient Morphological Image Analysis", Int. Conf. on Pattern Recogntion D: Parallel Computing, Vol. 94, pp. 257-261, 1994.
[7] S.Fejes, F.Vajda, "Efficient implementation technique of adaptive morphological operations", Mathematical Morphology and its Applications to Signal Processing II, ed. J.Serra and P.Soille, pp. 273-280, Kluwer Academic Publishers, The Netherlands, 1994.
[8] S.Fejes, F.Vajda, "A data-driven algorithm and systolic architecture for image morphology", Proc. Int. Conf. on Image Processing, Vol. II, pp. 550-554, 1994.
[9] G.Anelli, A.Broggi and G.Destri, "Decomposition of Arbitrarily Shaped Binary Morphological Structuring Elements Using Genetic Algorithms", IEEE Transactions on Pattern Analysis and Machine Intelligence, Vol. 20, No. 2, pp. 217-224, 1998.
[10] S.Loncaric, A.P.Dhawan, "Optimal Shape Description using Morphological Signature Transform via Genetic Algorithm", SPIE Proceedings 2030: Image Algebra and Morphological Image Processing, pp. 121-127, 1993.
[11] Z.Liposcak, S.Loncaric, "Face Recognition from Profiles Using Morphological Signature Transform", Proc. The 21st Int. Conf. on Information Technology Interfaces, pp. 93-98, 1999.
[12] T.Kikuchi, S.Murakami, "Application of Fuzzy Mathematical Morphology with Adaptive Structuring Elements to Seal Defect Testing", Journal of Advanced Computational Intelligence, Vol. 6, No. 1, pp. 62-69, 2002.
[13] H.Breu, J.Gil, D.Kirkpatrick and M.Werman, "Linear Time

Euclidean Distance Transform Algorithms", IEEE Transactions on Pattern Analysis and Machine Intelligence, vol. 17, no. 5, pp. 529-533, 1995.
[14] T.Hirata and T.Katoh, "An Algorithm for Euclidean distance transformation", SIGAL Technical Report of IPS of Japan, 94-AL-41-4, pp. 25-31, September, 1994.
[15] J. Serra and P. Soille, Mathematical Morphology and its Applications to Image Processing, Kluwer Academic Publishers, The Netherlands, 1994.
[16] G. Agam and Its'hak Dinstein, "Generalized Morphological Operators Applied to Map-Analysis", Proceedings of SSPE'96, pp. 60-69, 1996.
[17] X.F.Liang and T.Asano, "A fast denoising method for binary fingerprint image", Proc. The 4th IASTED Int. Conf. on VIIP, pp. 309-313, 2004.
[18] P.Viola and M.Jones, "Robust Real-time Face Dectection", International Journal of Computer Vision, Vol. 57(2), pp. 137-154, 2004.
[19] F.Crow, "Summed-area tables for texture mapping", Proceedings of SIGGRAPH, 18(3), pp. 207-212, 1984.
[20] F.Y.Shih and C.C.Pu, "A Skeletonization Algorithm by Maxima Tracking on Euclidean Distance Transform", Pattern Recognition, vol. 28, no. 3, pp. 331-341, March 1995.

Xuefeng Liang was born in 1974. He received the MS degree in computer science from Xi'dain University, China, in 2003, and is going to obtain PhD degree in information science from Japan Advanced Institute of Science and Technology in 2006. He is working on computational geometry, biometrics and image processing. He is also interested in intelligent algorithm.

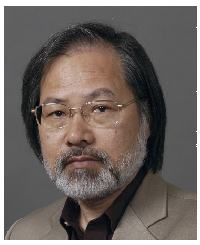

Dr. Tetsuo Asano was born in Kyoto Prefecture, Japan, in 1949. He got B.E., M.E., and Ph.D degrees from Osaka University, Japan, in 1972, 1974, and 1977, respectively. In 1977 he joined Osaka Electro-Communication University as a lecturer and moved to JAIST (Japan Advanced Institute of Science and technology) in 1997. He is now a professor in School of Information Science. His research interest includes algorithms and data structures, especially in computational geometry, combinatorial optimization, computer graphics, computer vision using geometric information, and VLSI layout design. He has been serving as editors of several journals including Discrete and Computational Geometry, Computational Geometry: Theory and Applications, International Journal of Computational Geometry and Applications, and Theory of Computing Systems. He served as a chair of a Special Interest Group on Algorithms of Information Processing Society of Japan in 1994-1996. He is fellows of Association of Computing Machinery (2001) and Information Processing Society of Japan (2004).